

One particle spectral weight of the three dimensional single band Hubbard model

M. Ulmke^{1*}, R. T. Scalettar¹, A. Nazarenko², and E. Dagotto²

1. Department of Physics, University of California, Davis, CA 95616

2. Department of Physics, and National High Magnetic Field Lab, Florida State University, Tallahassee, FL 32306
(January 24, 2018)

Dynamic properties of the three-dimensional single-band Hubbard model are studied using Quantum Monte Carlo combined with the maximum entropy technique. At half-filling, there is a clear gap in the density of states and well-defined quasiparticle peaks at the top (bottom) of the lower (upper) Hubbard band. We find an antiferromagnetically induced weight above the naive Fermi momentum. Upon hole doping, the chemical potential μ moves to the top of the lower band where a robust peak is observed. Results are compared with spin-density-wave (SDW) mean-field and self consistent Born approximation results, and also with the infinite dimensional ($D = \infty$) Hubbard model, and experimental photoemission (PES) for three dimensional transition-metal oxides.

I. INTRODUCTION

The single band two dimensional Hubbard Hamiltonian [1] has recently received considerable attention due to possible connections with high temperature superconductors. Indeed, evidence is accumulating that this Hamiltonian may describe, at least qualitatively, some of the normal state properties of the cuprates. [2] Exact Diagonalization (ED) and Quantum Monte Carlo (QMC) have been used to model static properties like the behavior of spin correlations and magnetic susceptibility both at half-filling and with doping. [2] Comparisons of dynamic quantities like the spectral weight and density of states with angle-resolved photoemission results [3–7] have also proven quite successful. Significantly, while analytic calculations have pointed towards various low temperature superconducting instabilities, such indications have been absent in numerical work. [2]

Historically, however, the Hubbard model was first proposed to model magnetism and metal-insulator transitions in 3D transition metals and their oxides, [1] rather than superconductivity. Now that the technology of numerical work has developed, it is useful to reconsider some of these original problems. A discussion of possible links between the 3D Hubbard model and photoemission results for YTiO_3 , SrVO_3 and others [8–10] has already recently occurred. In such perovskite Ti^{3+} and V^{4+} oxides, which are both in a $3d^1$ configuration, the hopping amplitude t between transition-metal ions can be varied by modifying the $d - d$ neighboring overlaps through a tetragonal distortion. Thus, the strength of the electron correlation U/t can be varied by changing the composition. In fact, a metal-insulator transition has been reported in the series $\text{SrVO}_3 - \text{CaVO}_3 - \text{LaTiO}_3 - \text{YTiO}_3$. On the metallic side, a quasiparticle band is experimentally observed near the Fermi energy E_F , as well as a high energy satellite associated to the lower Hubbard band (LHB). [8,16] Spectral weight is transferred from the quasiparticle to the LHB as U/t is increased at half-filling.

In this paper, we report the first use of Quantum

Monte Carlo, combined with analytic continuation techniques, to evaluate the spectral function and density of states for the 3D Hubbard Hamiltonian. The motivation is twofold. First, we want to compare general properties of the 3D Hubbard Hamiltonian with the extensive studies already reported in the literature [11,12,16,2] for the 2D and infinite-D cases. Of particular importance is the presence of quasiparticles near the half-filling regime, as well as the evolution of spectral weight with doping. Many of the high-Tc cuprates contain CuO_2 planes that are at least weakly coupled with each other, and thus the study of the 3D system may help in understanding part of the details of the cuprates. More generally, the Hubbard Hamiltonian is likely to continue being one of the models used to capture the physics of strongly correlated electrons, so we believe it is important to document its properties in as many environments as possible for potential future comparisons against experiments.

Secondly, we discuss a particular illustration of such contact between Hubbard Hamiltonian physics and experiments on 3D transition metal oxides. In addition to the studies of half-filled systems with varying correlation energy mentioned above, experiments where the band filling is tuned by changing the chemical composition have also been reported. [13,10,14] One compound that has been carefully investigated in this context is $\text{Y}_{1-x}\text{Ca}_x\text{TiO}_3$. At $x = 0$ the system is an antiferromagnetic insulator. As x increases, a metal-insulator transition is observed in PES studies. The lower and upper Hubbard bands (LHB and UHB) are easily identified even with x close to 1, which would naively correspond to small electronic density in the single band Hubbard model, i.e. a regime where U/t is mostly irrelevant. In the experiments, a very small amount of spectral weight is transferred to the Fermi energy, filling the gap observed at half-filling (i.e. generating a “pseudogap”).

Analysis of the PES results of these compounds using the paramagnetic solution of the Hubbard Hamiltonian in infinite-D [15], a limit where dynamic mean field theory becomes exact (see section II), has resulted in qualitative agreement [12,17,16] with the experimental results.

At and close to half-filling there is an antiferromagnetic (AF) solution which becomes unstable against a paramagnetic (PM) solution at a critical concentration of holes. In the PM case, weight appears in the original Hubbard gap as reported experimentally. However, this analysis of the spectral weight in terms of the infinite-D Hamiltonian is in contradiction with results for the density of states reported in the 2D Hubbard model [2] where it is found that upon hole (electron) doping away from half-filling the chemical potential μ moves to the top (bottom) of the valence (conduction) band. The results at $\langle n \rangle = 1$ in 2D already show the presence of a robust quasiparticle peak which is absent in the insulating PM solution of the $D = \infty$ model. That is, in the 2D system the large peak in the density of states observed away from half-filling seems to evolve from a robust peak already present at half-filling. On the other hand, at $D = \infty$ a feature resembling a “Kondo-resonance” is *generated* upon doping if the paramagnetic solution is used. This peak in the density of states does not have an analog at half-filling unless frustration is included. [12] Studies in 3D may help in the resolution of this apparent non-continuity of the physics of the Hubbard model when the dimension changes from 2 to ∞ . The proper way to carry out a comparison between $D = 3$ and ∞ features is to base the analysis on ground state properties. With this restriction, i.e. using the AF solution at $D = \infty$ and close to half-filling, rather than the PM solution, we found that the $D = 3$ and ∞ results are in good agreement.

In this paper we will consider which of these situations the 3D Hubbard Hamiltonian better corresponds to, and therefore whether the single band Hubbard Hamiltonian provides an adequate description of the density of states of 3D transition-metal oxides.

II. MODEL AND METHODS

The single band Hubbard Hamiltonian is

$$H = -t \sum_{\langle ij \rangle} (c_{i\sigma}^\dagger c_{j\sigma} + h.c.) - \mu \sum_{i\sigma} n_{i\sigma} + U \sum_i (n_{i\uparrow} - 1/2)(n_{i\downarrow} - 1/2), \quad (1)$$

where the notation is standard. Here $\langle ij \rangle$ represents nearest-neighbor links on a 3D cubic lattice. The chemical potential μ controls the doping. For $\mu = 0$ the system is at half filling ($\langle n \rangle = 1$) due to particle-hole symmetry. $t \equiv 1$ will set our energy scale.

We will study the 3D Hubbard Hamiltonian using a finite temperature, grand canonical Quantum Monte Carlo (QMC) method [18] which is stabilized at low temperatures by the use of orthogonalization techniques [19]. The algorithm is based on a functional-integral representation of the partition function obtained by discretizing the “imaginary-time” interval $[0, \beta]$ where β is the inverse

temperature. The Hubbard interaction is decoupled by a two-valued Hubbard-Stratonovich transformation [20] yielding a bilinear time-dependent fermionic action. The fermionic degrees of freedom can hence be integrated out analytically, and the partition function (as well as observables) can be written as a sum over the auxiliary fields with a weight proportional to the product of two determinants, one for each spin species. At half-filling ($\langle n \rangle = 1$), it can be shown by particle-hole transformation of one spin species ($c_{i\downarrow} \rightarrow (-1)^i c_{i\downarrow}^\dagger$) that the two determinants differ only by a positive factor, hence their product is positive definite. At general fillings, however, the product can become negative, and this “minus-sign problem” restricts the application of QMC to relatively high temperature (of order 1/30 of the bandwidth) off half-filling.

The QMC algorithm provides a variety of static and dynamic observables. One equal time quantity in which we are interested is the magnetic (spin-spin) correlation function,

$$C(\mathbf{l}) = \frac{1}{N} \sum_j \langle m_j m_{j+l} \rangle. \quad (2)$$

Here $m_j = \sum_\sigma \sigma n_{j\sigma}$ is the local spin operator, and N is the total number of lattice sites. Static correlations have also been investigated in earlier studies of the 3D Hubbard model [21,22] where the antiferromagnetic phase diagram at half filling was explored.

To obtain dynamical quantities in real time or frequency, the QMC results in imaginary time have to be analytically continued to the real time axis. Since we are mostly interested in the one-particle spectrum we measure the one-particle Green function $G(\mathbf{p}, \tau)$. The imaginary part of $G(\mathbf{p}, \omega)$ (in real frequency) defines the spectral weight function at momentum \mathbf{p} , $A(\mathbf{p}, \omega)$, which is related to $G(\mathbf{p}, \tau)$ by:

$$G(\mathbf{p}, \tau) = \int_{-\infty}^{\infty} d\omega A(\mathbf{p}, \omega) \frac{e^{-\tau\omega}}{1 + e^{\beta\omega}}. \quad (3)$$

$A(\mathbf{p}, \omega)$ can in principle be calculated by inverting Eq.(3), but the exponential behavior of the kernel at large values of $|\omega|$ makes this inversion difficult numerically. $G(\mathbf{p}, \tau)$ is quite insensitive to details of $A(\mathbf{p}, \omega)$ in particular at large frequencies. Since $G(\mathbf{p}, \tau)$ is known only on a finite grid in the interval $[0, \beta]$ and there only within the statistical errors given by the QMC-sampling, solving Eq.(3) for $A(\mathbf{p}, \omega)$ is an ill-posed problem. A large number of solutions exists, and the problem is to find criteria to select out the correct one. This can be done by employing the Maximum Entropy (ME) method [23]. Basically, the ME finds the “most likely” solution $A(\mathbf{p}, \omega)$ which is consistent with the data and all information that is known about the solution (like positivity, normalization, etc.). ME avoids “overfitting” to the data by a “smoothing” technique that tries to assimilate the resulting $A(\mathbf{p}, \omega)$ to a flat default model. In the absence of any data ($G(\mathbf{p}, \tau)$)

ME would converge to the default model which is chosen to be a constant within some large frequency interval. There is no adjustable parameter in the ME application. One needs accurate data for $G(\mathbf{p}, \tau)$ with a statistical error of $o(10^{-4})$ to get reliable results for $A(\mathbf{p}, \omega)$.

In principle, one can calculate analytically the first and second (and higher) moments of the spectral weight and include this information in the ME procedure. However, we chose to calculate the moments afterwards from the resulting function $A(\mathbf{p}, \omega)$, and to compare them with the analytically known results as a further test. The agreement was in all cases within 10%. Still, the ME methods provides only a rough estimate of the true spectral weight functions. Band gaps and the positions of significant peaks are usually well captured but fine structure which needs a high frequency resolution is hard to detect within the ME approach.

Integrating $A(\mathbf{p}, \omega)$ over the momenta gives the one-particle density of states (DOS) $N(\omega)$. However, technically, it is preferable to integrate first $G(\mathbf{p}, \tau)$, which reduces the statistical errors, and then perform the analytic continuation.

The DOS will be compared to results from the dynamical mean-field theory of infinite dimensions, $D = \infty$, [15]. In this limit, with the proper scaling of the hopping element ($t = t^*/\sqrt{Z}$, with Z being the coordination number) the one-particle self energy becomes local or, equivalently, momentum independent and the lattice problem is mapped onto a single site problem. The constant t^* is set to $t^* = \sqrt{6}$ to obtain the same energy scale, $t = 1$, when compared to the 3D case. [24] In contrast to conventional mean-field theories, the self energy remains frequency dependent, preserving important physics. Spatial fluctuations are neglected, an approximation which becomes exact in the limit $Z \rightarrow \infty$ ($Z = 2D$ for the simple cubic lattice). Even in $D = \infty$, the remaining local interacting problem cannot be solved analytically but will also be treated by a finite temperature QMC [25] supplemented by a self-consistency iteration [17,16]. The advantage is that the system can be investigated in the thermodynamic limit with a modest amount of computer time. Due to its local character the $D = \infty$ approach cannot provide information on momentum dependent spectral functions. However, recently a k -resolved spectral function has been studied [26] in $D = \infty$.

Among other things, the $D = \infty$ limit has been used recently to study the AF phase diagram in the Hubbard model [12]. The agreement of the Néel temperature with 3D results is good. [22] In $D = \infty$ it is further possible to suppress AF long range order artificially by restricting the calculation to the (at low temperatures unstable) paramagnetic solution at half-filling. In this way, one may simulate frustration due to the lattice structure or orbital degeneracy, although in the absence of calculations for hypercubic lattices with nearest and next-nearest uniform hopping amplitudes it is still a conjecture how close this approach is to including these effects fully.

III. HALF-FILLING

A. Quantum Monte Carlo

We first study the single particle spectral weight $A(\mathbf{p}, \omega)$ at relatively strong coupling, $U = 8$, and half-filling ($\langle n \rangle = 1$) at a low temperature of $T = 1/10$.

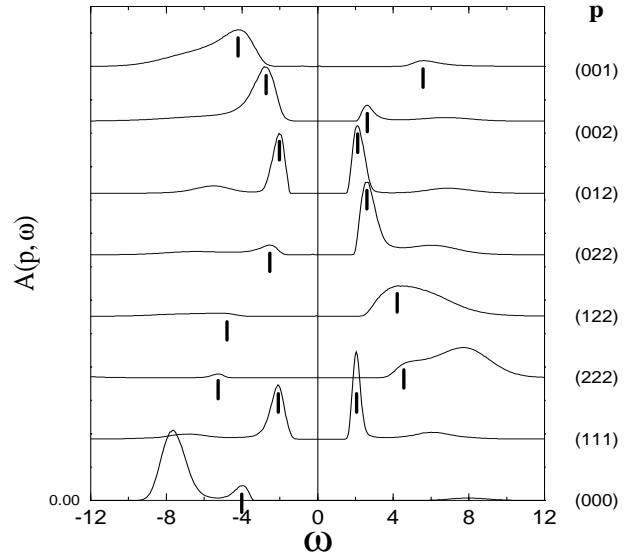


FIG. 1. Single particle spectral function $A(\mathbf{p}, \omega)$ versus ω for several momenta. The results correspond to a lattice with 4^3 sites, $U = 8$, $\beta = 10$, half-filling and using $t \equiv 1$ as energy scale. Momenta, \mathbf{p} , are in units of $\pi/2$. Bars indicate the position of the quasiparticle peak.

A gap is clearly present in the spectrum (Fig. 1) which is compatible with the expectation that the half-filled Hubbard model on a bipartite lattice is an antiferromagnetic insulator for all nonzero values of the coupling U/t . The spectral weight has four distinct features (two in the LHB and two identical ones in the UHB, as expected from particle-hole symmetry). In the UHB there is weight at a high energy, roughly in the interval between $\sim 5t$ and $8t$. This broad feature likely corresponds to the incoherent part of the spectral function found in previous simulations for the 2D Hubbard and $t - J$ models. [2] The dominant scale of this incoherent weight is t , and since it is located far from the top of the valence band its presence is not important for the low temperature properties of the system.

Much more interesting is the sharper peak found close to the gap in the spectrum. This band dispersion starts at a binding energy of approximately $\omega = -4t$ at momenta $(0, 0, 0)$ and moves up in energy obtaining its maximum value at $\omega \approx -2t$ at momenta $(0, \pi/2, \pi)$ and $(\pi/2, \pi/2, \pi/2)$ in Fig. 1. The width of the peak diminishes as the top of the valence band is reached. Similar structure was discussed before in studies of 2D systems, which had a somewhat higher resolution, as a “quasipar-

“particle” band corresponding to a hole moving coherently in an antiferromagnetic background. [2,27] This quasiparticle should be visualized as a hole distorting the AF order parameter in its vicinity. In this respect it is like a spin-polaron or spin-bag, [28] although “string states” likely influence its dispersion and shape. [2] The quasiparticle (hole plus spin distortion) movement is regulated by the exchange J , rather than t .

Using the center of the quasiparticle peaks of Fig. 1 as an indication of the actual quasiparticle pole position, we obtain a bandwidth W of about 2 to $3t$ or, equivalently, 4 to $6J$ using $J = 4t^2/U$ for $U = 8$. However, due to the low resolution of the ME procedure, reflected in part in the large width of the peaks of Fig. 1, it is difficult to show more convincingly within QMC/ME that the quasiparticle bandwidth is indeed dominated by J .

Note that moving from $(0,0,0)$ to (π,π,π) along the main diagonal of the Brillouin Zone (BZ), the PES part of the spectrum (i.e. the weight at $\omega < 0$) loses intensity. There is a clear transfer of weight from PES at small $|\mathbf{p}|$ to IPES at large $|\mathbf{p}|$, as observed in 2D simulations. [29] In addition, note that there is PES weight above the (naive) Fermi momentum of this half-filled system. For example, at $\mathbf{p} = (0,\pi,\pi)$, spectral weight at $\omega < 0$ can be clearly observed. Similarly, at $\mathbf{p} = (0,0,\pi)$ weight in the IPES region is found. This effective doubling of the size of the unit cell in all three directions is a consequence of the presence of AF long range order. The hole energy at $\mathbf{p} = (0,0,0)$ and (π,π,π) becomes degenerate in the bulk limit and the quasiparticle band, for example along the main diagonal of the BZ, has a reflection symmetry with respect to $(\pi/2,\pi/2,\pi/2)$, as observed in our results (Fig. 1). However, note that the actual intensity of the AF-induced PES weight close to (π,π,π) is a function of the coupling. As $U/t \rightarrow 0$, the intensity of the AF-induced region is also reduced to zero. The presence of this AF-generated feature has recently received attention in the context of the 2D high-T_c cuprates. [28,30] While its presence in PES experiments at optimal doping is still under discussion, these features clearly appear in PES experimental studies of half-filled insulators, like $\text{Sr}_2\text{CuO}_2\text{Cl}_2$. [31] Thus, while this behavior has been primarily discussed in the context of 2D systems angle-resolved PES (ARPES) studies of 3D insulators like LaTiO_3 might also show such features.

In Fig. 2 we show the density of states (DOS) $N(\omega)$ of the 4^3 lattice. The two features described before, namely quasiparticle and incoherent background, in both PES and IPES are clearly visible. Also shown in Fig. 2 is the temperature effect on $N(\omega)$ which is weak for the given temperatures ($\beta = 10$ and 4). The basic features are still retained, only the gap is slightly reduced and the quasiparticle peak less pronounced at the higher temperature.

Results corresponding to a larger coupling, $U = 12$, at $\beta = 4$ are shown in Fig. 3. The gap increases and the quasiparticle band becomes sharper as U/t grows, as expected if its bandwidth is regulated by J . $A(\mathbf{p},\omega)$ at $U = 12$, $\beta = 4$ are similar to the results shown in Fig. 1.

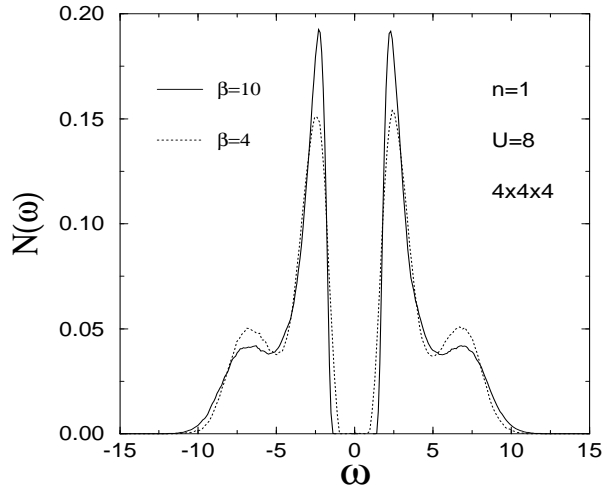


FIG. 2. Density of states $N(\omega)$ of the 3D Hubbard model on a 4^3 lattice, $U = 8$, $\beta = 10$ (solid line) and $\beta = 4$ (dashed line) and $\langle n \rangle = 1$. We do not enforce the $\rho(\omega) = \rho(-\omega)$ symmetry which occurs at half-filling due to particle-hole symmetry. However, deviations from this constraint are small, a further check on our numerics.

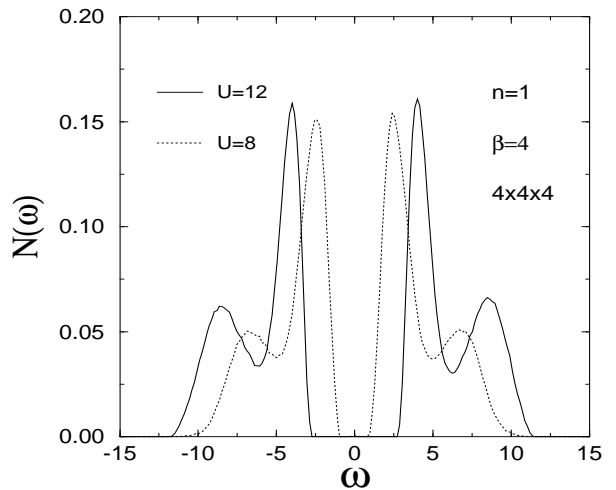


FIG. 3. Density of states $N(\omega)$ of the 3D Hubbard model on a 4^3 lattice at $U = 8$ (dashed line) and $U = 12$ (solid line), $\beta = 4$, and $\langle n \rangle = 1$.

A characteristic double peak like that seen in Figs. 2,3 has been observed in the X-ray absorption spectrum of LaFeO_3 [32], which is a strongly correlated, wide gapped antiferromagnetic insulator. The peaks appear at energies of about 2.2 eV and 3.8 eV. When Fe is substituted by Ni this structure vanishes and the system becomes a paramagnetic metal at a Ni concentration of about 80%. If we choose for comparison with the calculated DOS (Fig. 3) a hopping amplitude of $t = 0.5$ eV, giving a reasonable d-bandwidth of $W = 6$ eV, the positions of the quasiparticle peak and the maximum of the incoherent band for $U = 12t$ are at about $\omega_1 \approx 4t = 2$ eV

and $\omega_2 \approx 8.4t = 4.2$ eV, respectively. The agreement with the experimental values is fairly good considering the crude simplifications of the Hubbard model such as neglecting orbital degeneracy and charge transfer effects. Even the estimated charge gap of Fig. 3, defined by the onset of spectral weight relative to the Fermi energy, $\Delta_{charge} \approx 3t = 1.5$ eV is not too far from the experimental value of ~ 1.1 eV. The ratio $r = \omega_2/\omega_1$ decreases with U since for $U \gg t$ both energies are expected to converge to $U/2$. While for $U = 12t$, $r \approx 2.1$ is comparable to the experimental value (~ 1.7), it is too large for $U = 8$ ($r \approx 2.9$) showing that under the assumption of a single band Hubbard model description for LaFeO₃, the effective on-site interaction is at least of the size of the d-bandwidth.

Another feature which has been attributed to antiferromagnetic ordering was found in a high resolution PES study of V₂O₃. [33,34] In the AF insulator at $T = 100K$ the spectrum shows a shoulder at $\omega_1 = -0.8$ eV which is absent in the paramagnetic metal at $T = 200K$. This shoulder might be a reminiscent of the quasiparticle peak. The maximum of the lower Hubbard band is at about $\omega_2 \approx -1.3$ eV, giving a ratio $\omega_2/\omega_1 \approx 1.6$ similar to that observed in LaFeO₃. The on-site interaction was estimated to be about 1.5 times the bandwidth. [33]

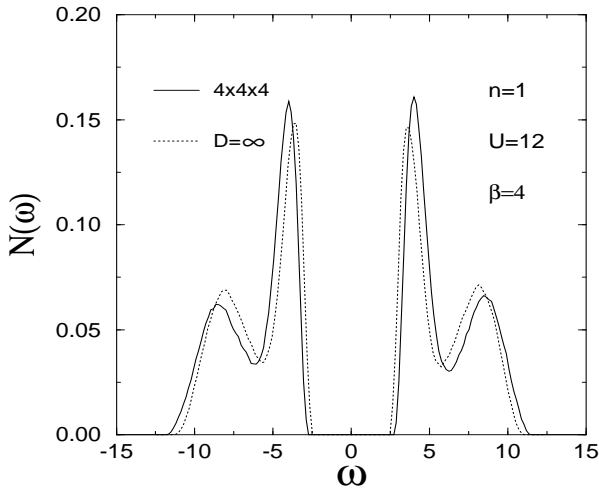


FIG. 4. Density of states $N(\omega)$ of the 3D Hubbard model on a 4^3 lattice at $U = 12$, $\beta = 4$ and $\langle n \rangle = 1$ (solid line) compared with the density of states at the same parameters for $D = \infty$ (dashed line).

It is interesting to compare the results obtained in our simulations with those found in the $D = \infty$ limit of the Hubbard model. At half-filling for arbitrary coupling strength, the $D = \infty$ model has an AF insulating ground state. Its DOS is shown in Fig. 4, using the same coupling and temperature as in the 3D simulation. $N(\omega)$ for both cases are similar, and they are also similar to results found before in 2D, suggesting that the physics of holes in an antiferromagnetic system is qualitatively the same irrespective of whether a 2D, 3D or ∞ D lattice is

used, at least within the accuracy of present QMC/ME simulations.

B. SDW mean-field and Born approximation

Since the data shown in the previous subsection correspond to holes in a system with AF long-range order, it is natural to compare our results against those found in mean-field approximations to the half-filled 3D Hubbard model that incorporate magnetic order in the ground state. The “spin-density-wave” mean-field approximation has been extensively used in the context of the 2D Hubbard model, [35] and here we will apply it to our 3D problem. For a lattice of N sites, the self-consistent equation for the gap Δ is

$$1 = \frac{U}{2N} \sum_{\mathbf{p}} \frac{1}{E_{\mathbf{p}}}, \quad (4)$$

where $E_{\mathbf{p}} = \sqrt{\epsilon_{\mathbf{p}}^2 + \Delta^2}$ is the quasiparticle energy, and $\epsilon_{\mathbf{p}} = -2t(\cos p_x + \cos p_y + \cos p_z)$ is the bare electron dispersion. The resulting quasiparticle dispersion is shown in Fig. 5 compared against the results of the QMC/ME simulation. The overall agreement is good if the coupling U in the gap equation Eq.(4) is tuned to a value $U \sim 5.6$. It is reasonable that a reduced U should be required for such a fit, since the SDW MF gap is usually larger than the more accurate QMC result. Similar renormalizations of U in comparing QMC and approximate analytic work has been discussed in the context of fitting the magnetic response, [36] and has also been explicitly calculated. [37] Fig. 5 shows many of the features observed in the numerical simulation, namely a hole dispersion which is maximized at $(\pi/2, \pi/2, \pi/2)$ for the momenta shown there, an overall bandwidth smaller than the noninteracting one, and the presence of AF-induced features in the dispersion above the naive Fermi momentum.

Thus the SDW MF approach qualitatively captures the correct hole quasiparticle bandwidth J at half-filling. However, a spurious degeneracy appears in the hole dispersion in this approximation. Momenta satisfying $\cos p_x + \cos p_y + \cos p_z = 0$ have the same energy. This is not induced by symmetry arguments and is an artifact of the SDW approach. In addition, $A(\mathbf{p}, \omega)$ in the SDW approximation only has one peak in the PES region for each value of the momentum, missing entirely the incoherent part.

While it may not be necessary to fix this problem in this case, it is important in general to be able to go beyond SDW MF. To do this, the self-consistent Born approximation [38] (SCBA) for one hole in the 3D $t - J$ model, which corresponds to the strong coupling limit of the Hubbard model, can be used. This technique reproduces accurately exact diagonalization results in the 2D case. [38]

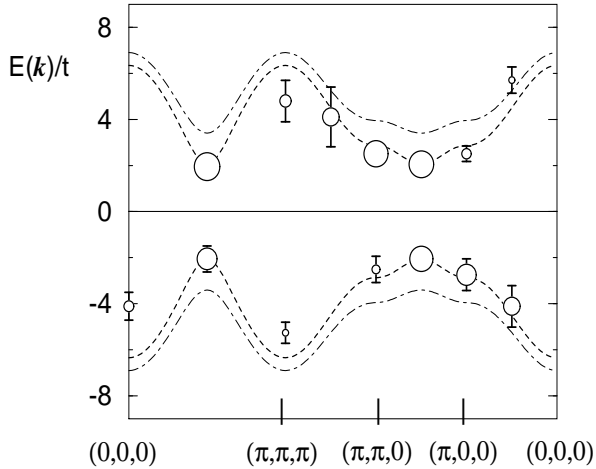


FIG. 5. Quasiparticle dispersion in the SDW MF approximation at half-filling and zero temperature. Results are at $U/t = 8$ (dot-dashed line) and $U = 5.57t$ (dashed line). QMC/ME results for the 3D Hubbard model on a 4^3 lattice at the same coupling, density and temperature are also shown (open circles). The area in the circles is proportional to the peak intensity. The error bars are the width of the peak. For some momenta the intensity of the PES or IPES data is so low that no peak position is reported.

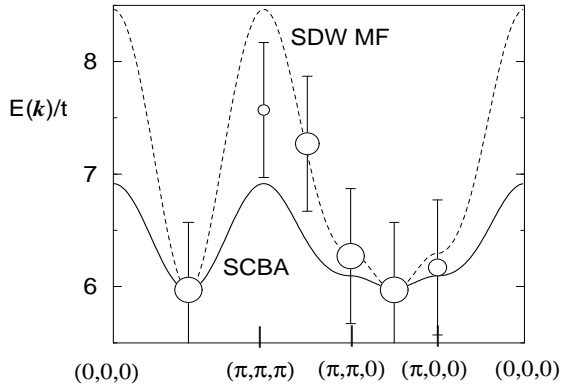


FIG. 6. Quasiparticle dispersion in the SDW MF approximation at $U = 12.8t$ (dashed line) compared against similar results obtained with the SCBA approximation for one hole in the $t - J$ model at $J/t = 0.3125$ (solid line). The energy scale of the SCBA dispersion is shifted such that the bottom of the band at $(\pi/2, \pi/2, \pi/2)$ agrees with the SDW MF result. The QMC data, also shown, lie between these weak and strong coupling approximations. The area in the circles is proportional to the peak intensity. The error bars are the width of the peak.

Actually, the dispersion of a dressed hole in an antiferromagnet within the SCBA for a bilayer system, and also for a 3D cubic lattice, has been recently studied. [39] Here, for completeness, we reproduce some of the results

of Ref. [39], and compare them against those of the 3D Hubbard model obtained with the SDW MF approximation and QMC calculations (Fig. 6). The comparison is carried out at $J/t \sim 0.3$ which corresponds to $U/t \sim 13$. The maximum of the dispersion in the valence band using the SCBA now lies at $(\pi/2, \pi/2, \pi/2)$, removing the spurious SDW MF degeneracy. In the scale of Fig. 6 the splitting between this momentum and $(\pi, \pi/2, 0)$ is difficult to resolve, since it corresponds to about 100K. Note that the bandwidth predicted by the SDW MF technique is approximately a factor two larger than the more accurate prediction of the SCBA. However, for this larger value of U it does not appear possible to fit simultaneously the SDW MF bandwidth and band-gap to the results of QMC by the same renormalization of U , something which can be done successfully at weaker coupling, $U = 8$. The QMC points at this intermediate coupling value where $U = \text{bandwidth}$ lie in between the SDW MF and SCBA. Though the uncertainties in the QMC results are rather large, we expect the agreement between SCBA and QMC results to improve as the coupling increases. The best fit of the SCBA data [39] is $\epsilon(\mathbf{p}) = c + 0.082(\cos p_x \cos p_y + \cos p_y \cos p_z + \cos p_x \cos p_z) + 0.022(\cos 2p_x + \cos 2p_y + \cos 2p_z)$ (eV), if $J = 0.125$ eV and $t = 0.4$ eV are used. The constant c is defined by the SDW MF gap (Fig. 6). As in the case of the 2D problem, holes tend to move within the same sublattice to avoid distorting the AF background. [2] Working at small J/t , the bandwidth of the 3D $t - J$ hole quasiparticle was found to scale as J , [39] as occurs in two dimensions.

IV. FINITE HOLE DENSITY

A. D=3

We can also use the QMC approach to study the 3D Hubbard model away from half-filling for temperatures down to about 1/30 of the bandwidth, a value for which $T \sim J$ for the present strong coupling values. First, we study the influence of doping and temperature on the spin-spin correlation function $C(\mathbf{l})$. At half filling $C(\mathbf{l})$ shows strong antiferromagnetic correlations over the whole 4^3 -lattice at $\beta = 10$ (Fig. 7). At $\beta = 2$ the correlations are significantly weakened, and with additional doping ($\langle n \rangle = 0.88$) all correlations are suppressed besides those between nearest neighbors. These appear to be stable against doping. The density of local moments, $\sqrt{C(0)}$ reaches its low temperature limit at an energy scale set by U and hence is unaffected by the change of β from $\beta = 2$ to $\beta = 10$ (note that longer range spin correlations form at a temperature set by the much smaller energy scale J). $\sqrt{C(0)}$ is to first order proportional to the electronic density and hence slightly reduced at $\langle n \rangle = 0.88$.

There has been considerable discussion concerning the

relationship between the spin-spin correlations and the presence of a gap in the density of states. In particular, it was observed [11] that if $N(\omega)$ is evaluated on lattices of increasing size at fixed temperature a well formed gap appearing on small lattices disappears when the spatial extent exceeds the spin-spin correlation length. Decreasing the temperature (and hence increasing the range of the spin correlation) allows the gap to reform. Similar effects are seen here in 3D.

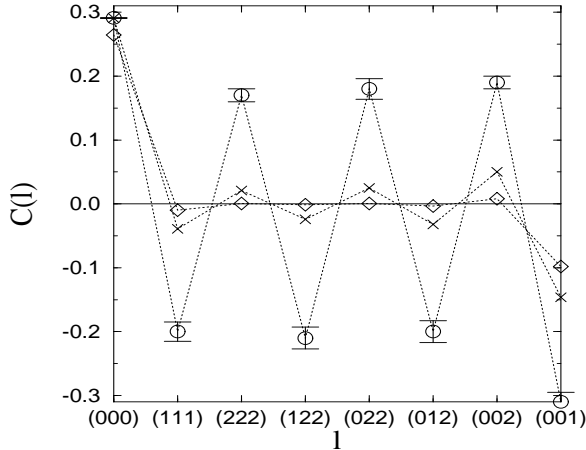


FIG. 7. Spin-spin correlation function $C(l)$ over a path in real space on the 4^3 lattice at $U = 8$, $\beta = 10$, $\langle n \rangle = 1$ (\circ); $\beta = 2$, $\langle n \rangle = 1$ (\times); and $\beta = 2$, $\langle n \rangle = 0.88$ (\diamond). $C(0)$ -values are divided by a factor of 3 for clearness. Error bars are smaller than the symbols when not shown.

Fig. 8a shows the density of states on a 4^3 lattice at several densities, $U = 8$ and $\beta = 2$. At this temperature the charge gap is not fully developed, and the quasiparticle peaks cannot be resolved. The result with doping is similar to that reported on 2D lattices. [40] The chemical potential μ moves to the top of the valence band as the density is reduced from half-filling. A large peak is generated which increases in intensity as $\langle n \rangle$ is further reduced. The weight of the upper part of the spectrum (reminiscent of the UHB) decreases with doping due to the reduced effective interaction. Similar results are shown in Fig. 8b but for a 6^3 lattice. There is not much difference between the two lattices, showing that within the resolution of the ME procedure finite size effects are small.

The large peak that appears in Fig. 8a-b at finite hole density is crossed by μ as the density is reduced. At $\langle n \rangle = 0.94$, the peak is located to the left of μ , at $\langle n \rangle = 0.88$ it has reached the chemical potential, and at $\langle n \rangle = 0.72$, the peak has moved to the right. This is in agreement with the behavior observed in both 2D QMC and ED simulations, [41] and it may be of relevance for estimations of superconducting critical temperatures if a source of carrier attraction is identified. [42]

The results of the previous section at half-filling obtained at low temperatures ($T \sim 1/10$) revealed a sharp

quasiparticle peak in the DOS at the top of the valence band and bottom of the conduction band. Numerical studies of 2D lattices have shown that the peak intensity at $T = 0$ is the *largest* at half-filling. [41] Away from half-filling, the peak is still visible but it is broader than at $\langle n \rangle = 1$. [41] Thus there is no evidence that the sharp peak in the DOS of the doped system has been generated dynamically and represents a “Kondo-resonance” induced by doping, as has sometimes been suggested [12], and as Fig. 8 obtained at relatively high temperature, $\beta = 2$, seem to imply.

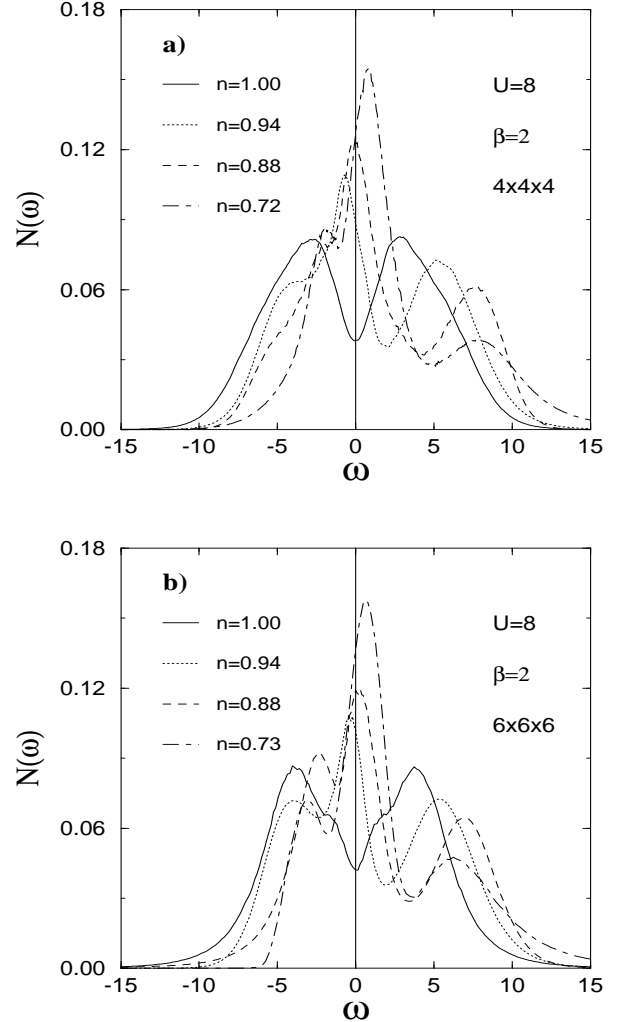


FIG. 8. (a) $N(\omega)$ for the 3D Hubbard model on a 4^3 lattice with $U = 8$ and $\beta = 2$ at several densities indicated in the figure; (b) same as (a) but on a 6^3 lattice. Frequencies are always relative to the chemical potential μ .

Another important quantity to study is the quasiparticle residue Z . The SCBA results show that Z is small but finite for the case of one hole in an antiferromagnetic insulator state, and actually the results are very similar in 3D and 2D systems. [38,39] Numerical results provide

a similar picture. [2] On the other hand, Z vanishes in the $D = \infty$ approach working in the paramagnetic state as the doping δ tends to zero. Note that in this state there are no AF correlations ($\xi_{AF} = 0$). Thus, it is clear that the hole quasiparticle at half-filling observed in the 2D and 3D systems is *not* related with the quasiparticle-like feature observed in the PM state at $D = \infty$.

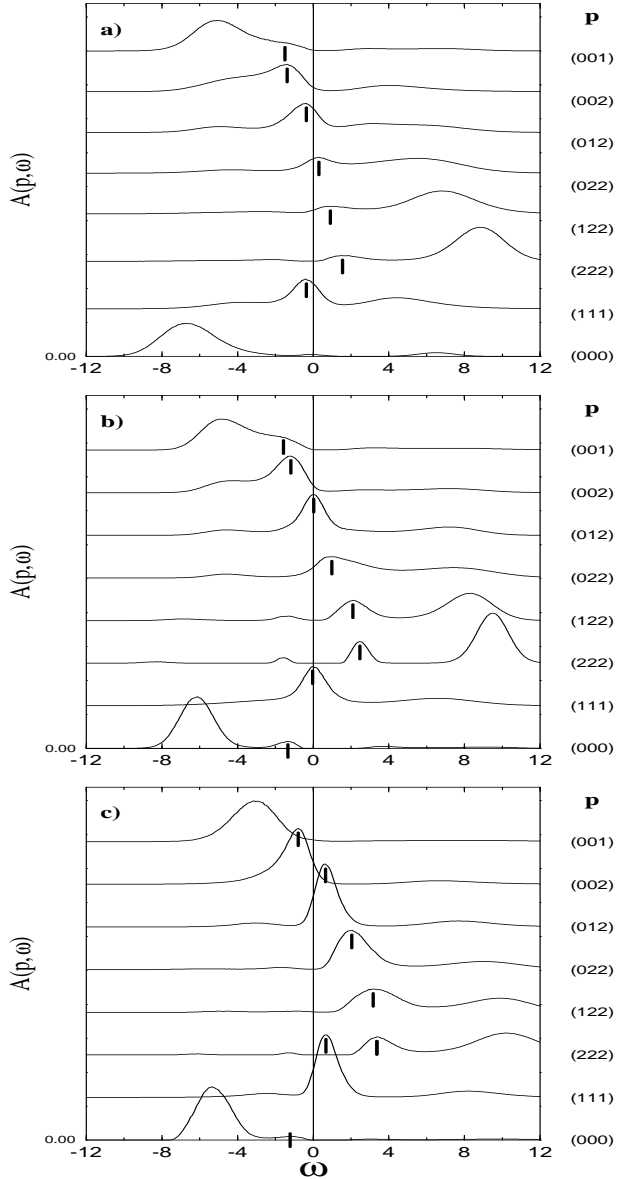


FIG. 9. (a) Spectral weight $A(\mathbf{p}, \omega)$ of the 3D Hubbard model calculated using QMC/ME on a 4^3 lattice, at $U = 8$, $\beta = 2$, and at density $\langle n \rangle = 0.94$; (b) same as (a) but at $\langle n \rangle = 0.88$; (c) same as (a) but at $\langle n \rangle = 0.72$.

In Fig. 9, we show $A(\mathbf{p}, \omega)$ obtained on the 4^3 lattice, $U = 8$, $T = 1/2$ and various densities away from half-filling. The gap is now absent. From the energy location of the maximum of the dominant peak in Fig. 9a-c, the quasiparticle dispersion can be obtained. The results are

shown in Fig. 10. It is remarkable that the quasiparticle dispersion resembles that of a noninteracting system i.e. $\epsilon_{\mathbf{p}} = -2t^*(\cos p_x + \cos p_y + \cos p_z)$, with a scale increasing from $t^* \sim t/4$ to $t/3$ with doping. This dispersion certainly does not exhaust all the spectral weight but a large incoherent part still remains at this coupling, density and temperature. Similar results were observed in 2D. [5,27,41,43] Only vestiges remain of the AF induced weight in PES near (π, π, π) . However, this drastic reduction of the AF induced intensity may be caused by the high temperature of the simulation as observed in the spin-spin correlation function (Fig. 7).

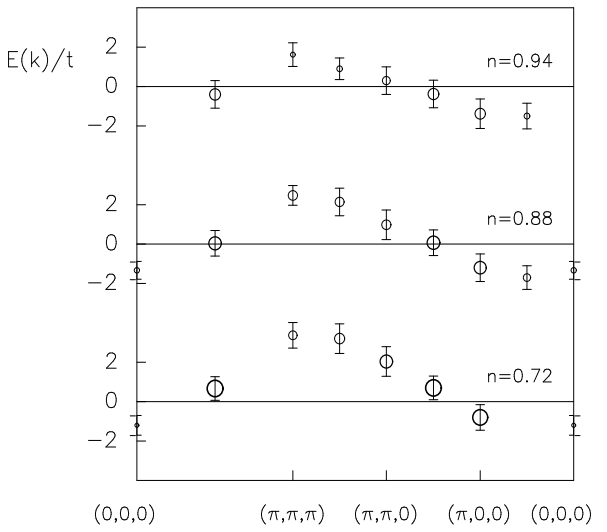


FIG. 10. Dispersion of the dominant peak of Fig. 9a-c against momentum. The densities are indicated. The area in the circles is proportional to the peak intensity. Error-bars correspond to the half-width of the peaks in the spectral weight.

B. $D = \infty$

The previous subsection and the results at half-filling have shown that the DOS of the 3D Hubbard model has a large peak at the top of the valence band. The peak is crossed by the chemical potential as $\langle n \rangle$ decreases. This behavior is in apparent contradiction with results reported at $D = \infty$ where a peak is generated upon doping if the “paramagnetic” solution to the mean-field problem is selected. At $D = \infty$, there are only two very distinct magnetic ground states. One has AF long-range order, and the other is a paramagnet with strictly zero AF correlation length i.e. without short range antiferromagnetic fluctuations. Thus, at $D = \infty$ the transition is abrupt from a regime with $\xi_{AF} = \infty$ to $\xi_{AF} = 0$. This does not occur in finite dimensions where before the long-range order regime is reached, AF correlations start building

up smoothly. This qualitative difference is depicted in Fig. 11.

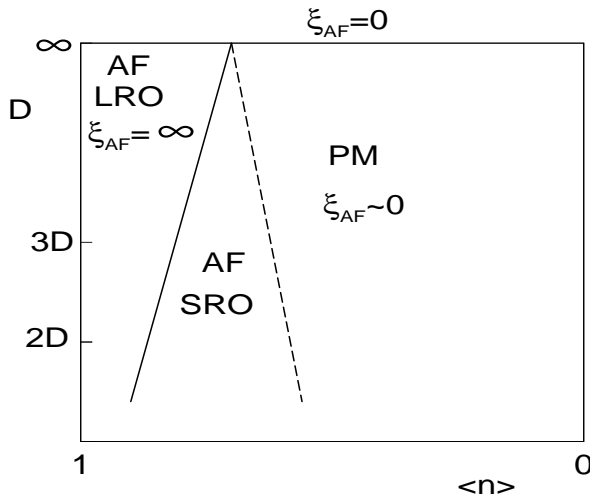


FIG. 11. “Phase diagram” of the Hubbard model (1) in the D - $\langle n \rangle$ -plane. Solid line: AF phase boundary; dashed line: crossover where short range AF correlations disappear. The intermediate regime of short range AF order vanishes in the limit $D \rightarrow \infty$.

ξ_{AF} as small as a couple of lattice spacings can be robust enough to induce important changes in the carrier dispersion, and may even be enough to induce superconductivity as many theories for the 2D high- T_c cuprates conjecture. We believe that the absence of a regime of intermediate size AF correlations at large D is the key ingredient that explains the differences reported here between $D=2,3$ and $D=\infty$.

In Fig. 12a, the $D=\infty$ DOS in the AF phase is shown at $\langle n \rangle = 1$ and 0.94. For these densities the AF-phase is energetically stable. We observe the tendency of the large peak at the bottom of the valence band to move towards the chemical potential in good agreement with the 3D Quantum Monte Carlo simulations. As found in 2D, the intensity of the peak decreases as we move away from half-filling if the temperature is low enough. In Fig. 12b, the DOS in the $D = \infty$ limit working in the paramagnetic phase is shown at several densities. For the present interaction, $U = 8$, the paramagnetic solution remains metallic at all temperatures even at half filling. [12] The results are qualitatively different from those observed in the AF regime. At $\langle n \rangle = 1$ a large peak at the chemical potential is clearly visible. Upon hole doping this peak gradually moves toward higher energies. At sufficiently strong doping the DOS of the PM-phase (Fig. 12b) resembles the results for the 3D lattices (Fig. 8), which is not surprising since AF correlations in 3D are strongly suppressed at the present temperature. Close to half filling, however, the 3D results are closer to the DOS of the AF-phase where a strong peak is observed on the left hand side of the chemical potential μ . This result is

gratifying since the proper way to compare $D = 3$ and ∞ results is by using the actual ground states in each dimension. In $D = \infty$, at low temperatures, the crossing of the peak by μ is expected at that point where the AF-Phase becomes unstable against doping.

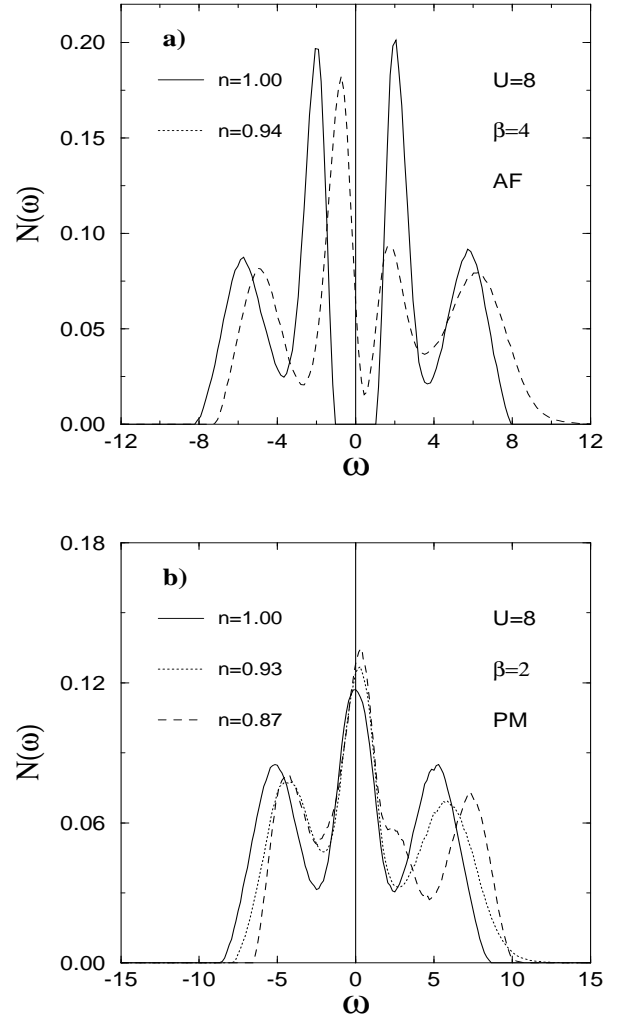


FIG. 12. (a) $N(\omega)$ corresponding to the $D = \infty$ Hubbard model at $U = 8$, $\beta = 4$ at the electronic densities indicated. The results were obtained using the AF solution to the mean-field equation; (b) same as (a) but using $\beta = 2$ and the PM solution to the mean-field equation.

V. CONCLUSIONS

In this paper we have calculated the single particle properties of the 3D single band Hubbard model using Quantum Monte Carlo and the SDW mean field and SCBA approximations. Our results have many similarities with those reported previously in 2D systems. At half-filling, peaks at the top of the valence band and bottom of the conduction band are observed in the DOS.

Their behavior is associated with spin polarons with a bandwidth of order the exchange J . We found similarities to and semi-quantitative agreement with experimentally observed features in the spectra of strongly correlated 3D AF insulators, LaFeO_3 and V_2O_3 .

As we dope the system, the sharp peak associated with these quasiparticles is crossed by the chemical potential as the density $\langle n \rangle$ changes. The PES weight observed away from half-filling is already present at half-filling. No new states are generated by doping. This result must be contrasted with that observed experimentally in, e.g., $\text{Y}_{1-x}\text{Ca}_x\text{TiO}_3$ using angle-integrated PES. In this case spectral weight which is not present in the insulator appears at E_F in the metallic regime as we dope the system. This behavior does not seem reproduced by the single band Hubbard model Eq.(1) in 3D, whose physics appears to be very close to that of 2D. Indeed for the 2D cuprates it has been shown experimentally that the states found at E_F upon doping are already present at half-filling. [44]

An exception among 3D materials is $\text{NiS}_{2-x}\text{Se}_x$ which remains antiferromagnetic throughout the metal-insulator transition induced by (homovalent) Se-substitution or temperature. PES spectra at $x = 0.5$ for different temperatures [45] show a strong peak close to the Fermi energy which does *not* disappear in the insulator. Instead the peak is shifted off the Fermi energy and only very slightly reduced in weight. Since this situation is not described within the paramagnetic $D = \infty$ approach, AF correlations are presumably essential for the low energy electronic excitations of this system.

The success of the $D = \infty$ approach to the Hubbard model in describing the physics of $\text{Y}_{1-x}\text{Ca}_x\text{TiO}_3$, SrVO_3 and CaVO_3 , however, appears crucially to depend upon forcing the paramagnetic solution of the equations. [46] In this case, states are actually *generated* in the Hubbard gap after a small hole doping is introduced. Of course, it may be that the “arbitrary” choice of this paramagnetic solution, which is not the actual minimum of the free energy, is well motivated since it mimics the presence of physical effects like frustration which destroy long range order in real materials. More work is needed to show that this scenario is realized for realistic densities and couplings.

An alternative explanation for the discrepancy between the PM solution in infinite-D and finite dimensional results may lie in the finite resolution of the combination of Monte Carlo simulations and Maximum Entropy techniques. However, the SCBA and results at half-filling and low T show that it is likely that at $\langle n \rangle = 1$ we have quasiparticle states in the DOS.

In studies of the single band Hubbard Hamiltonian in 2D, and in the present analysis in 3D, it is clear that short-range AF correlations play an important role close to $\langle n \rangle = 1$. In particular, the states created at the top of the valence band are likely to be spin polarons with a finite quasiparticle residue Z . PES states observed at finite hole doping evolve continuously from those present

at half-filling. Experiments on the 2D high-Tc cuprates seem to present similar features, while the results for the 3D perovskites are very different in the sense that no remnants of the coherent part of the spectrum away from half-filling are reported at half-filling.

Still, strong AF correlations are apparently present in several 3D transition metal oxides and influence the low energy spectrum at least on the insulating side of the transition. The introduction of frustration in the single band Hubbard model in 3D, perhaps through next-nearest neighbor hoppings, will reduce AF correlations and in particular the AF-induced charge gap, and might be sufficient to observe a evolution of spectral weight upon doping closer to the experimental findings. However, it might be that 3D models which explicitly include orbital degeneracy will be necessary to reproduce the physics of the transition metal oxides, as has recently been described for NiO chains [47] and Mn-oxides. [48]. Indeed, a recent argument presented by Kajueter et al. [49] to justify the use of the $D = \infty$ model provides a more realistic explanation for the apparent link between theory in this limit, and 3D transition-metal oxide results. The idea is that the physics of the real perovskite 3D oxides is influenced by the orbital degeneracy. Presumably this effect leads to a drastic reduction of the antiferromagnetic correlations that dominate the physics of these 2D and 3D systems. Many orbitals, including Hund’s coupling, produce an effective magnetic frustration that may reduce the AF correlation length to a negligible value even close to the AF insulator at half-filling. Such a frustration effect could be strong enough to generate a finite critical coupling U/t at half-filling.

VI. ACKNOWLEDGMENTS

We thank A. Fujimori, M. Rozenberg and A. Moreo for useful discussions. We are grateful to A. Sandvik for providing his Maximum Entropy program. Most simulations were done on a cluster of HP-715 work stations at the Electrical and Computer Engineering Department at UC Davis. We thank P. Hirose and K. Runge for technical assistance. E. D. is supported by grant NSF-DMR-9520776. R. T. S. is supported by grant NSF-DMR-9528535. M. U. is supported by a grant from the Office of Naval Research, ONR N00014-93-1-0495 and by the Deutsche Forschungsgemeinschaft. We thank the National High Magnetic Field Laboratory (NHMFL) and the Center for Materials Research and Technology (MARTECH) for additional support.

* New address: Theoretische Physik III, Universität Augsburg, D-86135 Augsburg, Germany.
 Electronic address: ulmke@physik.uni-augsburg.de

[1] M.C. Gutzwiller, Phys. Rev. Lett. **10**, 159 (1963); J. Hubbard, Proc. Roy. Soc. **A 276**, 238 (1964); J. Kanamori, Prog. Theor. Phys. **30**, 275 (1963).

[2] E. Dagotto, Rev. Mod. Phys. **66**, 763 (1994), and references cited therein.

[3] D.S. Dessau et al., Phys. Rev. Lett. **71**, 2781 (1993); K. Gofron et al., Phys. Rev. Lett. **73**, 3302 (1994).

[4] E. Dagotto, A. Nazarenko and M. Boninsegni, Phys. Rev. Lett. **73**, 728 (1994).

[5] N. Bulut, D.J. Scalapino and S.R. White, Phys. Rev. **B50**, 7215 (1994).

[6] R. Preuss, W. Hanke, and W. von der Linden, Phys. Rev. Lett. **75**, 1344 (1995).

[7] M. Langer, J. Schmalian, S. Grabowski, and K.H. Bennemann, Phys. Rev. Lett. **75**, 4508 (1995).

[8] A. Fujimori, I. Hase, H. Namatame, Y. Fujishima, Y. Tokura, H. Eisaki, S. Uchida, K. Takegahara, and F. M. F. de Groot, Phys. Rev. Lett. **69**, 1796 (1992).

[9] I. H. Inoue, I. Hase, Y. Aiura, A. Fujimori, Y. Haruyama, T. Maruyama, and Y. Nishihara, Phys. Rev. Lett. **74**, 2539 (1995).

[10] K. Morikawa, T. Mizokawa, K. Kobayashi, A. Fujimori, H. Eisaki, S. Uchida, F. Iga, and Y. Nishihara, Phys. Rev. **B 52**, 13711 (1995).

[11] M. Vekic and S.R. White, Phys. Rev. **B47**, 1160 (1993); G.S. Feng and S.R. White, Phys. Rev. **B46**, 8691 (1992); and M. Vekic and S.R. White, Phys. Rev. **B47**, 5678 (1992).

[12] M. Jarrell and T. Pruschke, Z. Phys. **B 90**, 187 (1993).

[13] A. Fujimori, I. Hase, M. Nakamura, H. Namatame, Y. Fujishima, Y. Tokura, M. Abbate, F. M. F. de Groot, J. C. Fuggle, O. Strelbel, M. Doce, and G. Kaindl, Phys. Rev. **B 46**, 9841 (1992).

[14] Y. Tokura, Y. Taguchi, Y. Okada, Y. Fujishima, T. Arima, K. Kumagai, and Y. Iye, Phys. Rev. Lett. **70**, 2126 (1993).

[15] W. Metzner and D. Vollhardt, Phys. Rev. Lett. **62**, 324 (1989); for a review see D. Vollhardt, in *Correlated Electron Systems*, ed. V. J. Emery (World Scientific, Singapore, 1993), p. 57.

[16] For a review see A. Georges, G. Kotliar, W. Krauth, and M. Rozenberg, Rev. Mod. Phys. **68** 13 (1996).

[17] For a review see Th. Pruschke, M. Jarrell, and J. K. Freericks, Adv. Phys. **44**, 187 (1995).

[18] R. Blankenbecler, D. J. Scalapino, R. L. Sugar, Phys. Rev. **D 24**, 2278 (1981).

[19] S. R. White, D. J. Scalapino, R. L. Sugar, E. Y. Loh, J. E. Gubernatis, R. T. Scalettar, Phys. Rev. **B 40**, 506 (1989).

[20] J. E. Hirsch, Phys. Rev. **B 28**, 4059 (1983).

[21] J. E. Hirsch, Phys. Rev. **B 35**, 1851 (1987).

[22] R. T. Scalettar, D. J. Scalapino, R. L. Sugar and D. Toussaint, Phys. Rev. **B 39**, 4711 (1989).

[23] For a review see M. Jarrell and J. E. Gubernatis, Phys. Rep. **269**, 133 (1996).

[24] We choose a half-elliptic, non-interacting density of states which becomes exact for the Bethe lattice with infinite connectivity. Like real 3D-DOS and in contrast to the hypercubic lattice in $D = \infty$ it has a finite bandwidth ($W = 4t^*$) and algebraic band edges.

[25] J. E. Hirsch and R. M. Fye, Phys. Rev. Lett. **56**, 2521 (1986).

[26] M. Rozenberg, G. Kotliar, and H. Kajueter, preprint.

[27] A. Moreo et al., Phys. Rev. **B 51**, 12045 (1995).

[28] A. Kampf and J. R. Schrieffer, Phys. Rev. **B 41**, 6399 (1990).

[29] N. Bulut, D. J. Scalapino, and S. R. White, Phys. Rev. Lett. **73**, 748 (1994).

[30] P. Aebi et al., Phys. Rev. Lett. **72**, 2757 (1994); S. Haas et al., Phys. Rev. Lett. **74**, 4281 (1995).

[31] B.O. Wells, et al., Phys. Rev. Lett. **74**, 964 (1995).

[32] D. D. Sarma et al., Phys. Rev. **B 49**, 14238 (1994).

[33] S. Shin et al., J. Phys. Soc. Jpn. **64**, 1230 (1994).

[34] M.J. Rozenberg, G. Kotliar, H. Kajueter, G.A. Thomas, D.H. Rapkine, J.M. Honig, and P. Metcalf, Phys. Rev. Lett. **75** 105, 1995.

[35] J. R. Schrieffer, X. G. Wen, and S. C. Zhang, Phys. Rev. **B 39**, 11663 (1989).

[36] N. Bulut, D.J. Scalapino, and S.R. White, Phys. Rev. **B47**, 14599 (1993).

[37] P. van Dongen, Phys. Rev. Lett. **67**, 757 (1991). The self-consistent perturbation theory around the SDW MF solution provides a renormalization factor about $q = 0.29$ in the limit of small U in $D = 3$ and $D = \infty$. Numerically it was found that q increases with U , see e.g. [12].

[38] S. Schmitt-Rink, C.M. Varma, and A.E. Ruckenstein, Phys. Rev. Lett. **60**, 2793 (1988); F. Marsiglio, A.E. Ruckenstein, S. Schmitt-Rink, and C.M. Varma, Phys. Rev. **B43**, 10882 (1991); G. Martinez and P. Horsch, Phys. Rev. **B44**, 317 (1991); Z. Liu and E. Manousakis, Phys. Rev. **B45**, 2425 (1992).

[39] A. Nazarenko and E. Dagotto, preprint.

[40] N. Bulut, D.J. Scalapino and S.R. White, Phys. Rev. Lett. **72**, 705 (1994).

[41] A. Nazarenko, S. Haas, J. Riera, A. Moreo, and E. Dagotto, preprint.

[42] Recently proposed theories of high-Tc make extensive use of a large accumulation of weight in the DOS near the chemical potential to enhance the critical temperature [E. Dagotto, A. Nazarenko and A. Moreo, Phys. Rev. Lett. **74**, 310 (1995)].

[43] E. Dagotto, F. Ortolani and D. Scalapino, Phys. Rev. **B 46**, 3183 (1992).

[44] A. Fujimori et al., Phys. Rev. **B 39**, 2255 (1989); Phys. Rev. **B 40**, 7303 (1990).

[45] A. Y. Matsuura, Z.-X. Shen, D. S. Dessau, C.-H. Park, T. Thio, J. W. Bennett, O. Jepson, Phys. Rev. **B 53**, R7584 (1996).

[46] M. J. Rozenberg , I. H. Inoue , H. Makino , F. Iga , Y.

[47] E. Dagotto, J. Riera, A. Sandvik, and A. Moreo, Phys. Rev. Lett. **76**, 1731 (1996).

[48] E. Müller-Hartmann and E. Dagotto, preprint.

[49] H. Kajueter, G. Kotliar, and G. Moeller, preprint Rutgers Univ. (1996).